Protein Farnesyltransferase: Kinetics of Farnesyl Pyrophosphate Binding and Product Release

Eric S. Furfine,*,‡ Johann J. Leban,§ Anthony Landavazo,§ John F. Moomaw,|| and Patrick J. Casey||

Divisions of Experimental Therapy and Organic Chemistry, Wellcome Research Laboratories, 3030 Cornwallis Road, Research Triangle Park, North Carolina 27709, and Department of Molecular Cancer Biology, Duke University Medical Center, Durham, North Carolina 27710

Received November 7, 1994; Revised Manuscript Received February 22, 1995[⊗]

ABSTRACT: Protein farnesyltransferase (FTase) catalyzes the prenylation of Ras and several other key proteins involved in cell regulation. The mechanism of the FTase reaction was elucidated by pre-steady-state and steady-state kinetic analysis. FTase catalyzed the farnesylation of biotinylated peptide substrate (BiopepSH) by farnesyl pyrophosphate (FPP) to an *S*-farnesylated peptide (BiopepS-C_{15}). The steady-state kinetic mechanism was ordered. FTase bound FPP in a two-step process with an effective dissociation rate constant of 0.013 s^{-1} and an overall K_d of 2.8 nM. BiopepSH reacted with FTase·FPP irreversibly, with a second-order rate constant of 2.2×10^5 M^{-1} s^{-1}, to form FTase·BiopepS-C_{15}. Because most of the FPP in FTase·FPP was trapped as FTase·BiopepS-C_{15} at high concentrations of BiopepSH, FPP dissociated slowly from the ternary complex relative to catalysis, so that the commitment to catalysis was high. The maximal rate constant for formation of FTase·BiopepS-C_{15} (enzyme-bound product) is much larger than k_{cat} (0.06 s^{-1}), indicating that product release is the rate-determining step in the reaction mechanism.

Protein farnesyltransferase (FTase)[1] catalyzes the *S*-farnesylation of cysteine residues in protein substrates by farnesyl pyrophosphate (FPP). The active cysteine is the fourth residue from the COOH-terminus in the consensus sequence Cys-aaX, where "a" is any of several amino acids, and "X" is generally methionine, serine, or glutamine (Clarke, 1992; Reiss et al., 1991b). Substrates for FTase include Ras proteins, nuclear lamins, and several proteins involved in visual signal transduction (Clarke, 1992; Casey, 1994). FTase also binds short peptides with appropriate Cys-aaX sequences (Reiss et al., 1990, 1991b; Goldstein et al., 1991); this binding site has been exploited in design of peptidomimetic inhibitors of the enzyme. Such inhibitors reverse transformation of cells by oncogenic forms of Ras (Kohl et al., 1993; James et al., 1993) and, in one instance, exhibit efficacy in an animal model (Kohl et al., 1994). These results support the emerging view that FTase is a prime target for development of anticancer therapeutics (Gibbs et al., 1994).

FTase has been purified to homogeneity from rat brain and bovine brain cytosol using peptide affinity chromatography (Reiss et al., 1990; Moores et al., 1991). The enzyme has two nonidentical subunits, designated α and β, with apparent molecular masses of approximately 48 and 46 kDa, respectively. The amino acid sequences of both subunits have been deduced from their cDNA sequences (Chen et al., 1991a,b; Kohl et al., 1991). Substantial quantities of purified protein can be readily produced by high-level expression of recombinant FTase in bacterial (Omer et al., 1993) and eukaryotic (Chen et al., 1993) cells.

Steady-state kinetic analysis of FTase indicated a formally random but functionally ordered sequential mechanism for the enzyme (Pompliano et al., 1992), whereby the preferred pathway for catalysis involves FPP binding first (Pompliano et al., 1993). This mechanism is consistent with findings that mammalian FTase binds an immobilized substrate peptide in the absence of FPP (Reiss et al., 1990) and that the enzyme forms a complex with FPP in the absence of protein substrate (Reiss et al., 1991a). The maximal turnover number of FTase (k_{cat}) is 1 min^{-1} (Reiss et al., 1990; Pompliano et al., 1992). In this steady-state analysis, the rate-limiting step in the overall reaction was proposed to include conversion of the ternary complex to enzyme−product complex. However, the possibility that k_{cat} was a result of slow release of product was not addressed. Because questions such as this are difficult to answer by steady-state kinetic analysis, we have conducted a detailed pre-steady-state analysis of FTase. Our results indicate that product release limits the overall rate of the FTase reaction. Additionally, we have found that FTase binds FPP in a two-step process.

MATERIALS AND METHODS

Materials. Unlabeled FPP was from USF (Tampa, FL), [1-^{3}H]FPP was from DuPont New England Nuclear Research Products (Wilmington, DE), assay stop reagent and streptavidin-coated scintillation beads were part of an FTase assay kit from Amersham Corporation (Arlington Heights, IL), alkaline phosphatase (ammonium sulfate suspension) and Triton X-100 were from Sigma (St. Louis, MO), biotinylated-GLPCVVM was prepared by standard procedures (Merri-

* To whom correspondence should be addressed.
‡ Division of Experimental Therapy, Wellcome Research Laboratories.
§ Division of Organic Chemistry, Wellcome Research Laboratories.
|| Duke University Medical Center.
⊗ Abstract published in *Advance ACS Abstracts,* May 1, 1995.
[1] Abbreviations: FTase, protein farnesyltransferase; FPP, farnesyl pyrophosphate; BiopepSH, biotinyl-GLPCVVM; BiopepS-C_{15}, *S*-farnesylbiotinyl-GLPCVVM farnesylated at the cysteine residue; Tris, tris(hydroxymethyl)aminomethane; EDTA, ethylenediaminetetraacetic acid; SPA, scintillation proximity assay; BSA, bovine serum albumin; DMSO, dimethyl sulfoxide; DTT, dithiothreitol.

0006-2960/95/0434-6857$09.00/0

field, 1963; Stewart & Young, 1984), and recombinant FTase was prepared as described by Chen et al. (1993).

Enzyme Assay. FTase was assayed with the SPA assay kit. FTase (0.25−300 nM) was incubated for defined times with 0.025−4 μM BiopepSH, 2−220 nM FPP, 5 mM $MgCl_2$, 5 μM $ZnCl_2$, 2% DMSO, 0.01% Triton X-100, and 2 mM DTT in 25−200 μL of 50 mM Tris, pH 7.7, at 25 °C. Reactions were quenched with at least 2 vol of a suspension of 0.7 mg/mL scintillation beads (110 pmol of avidin/mg of beads) in stop reagent (0.75 M $MgCl_2$, 0.1 M NaH_2PO_4, pH 4.0, 0.5% BSA, and 0.05% sodium azide). A sufficient volume of bead/stop reagent mixture was used such that all of the biotinylated peptide in the solution was bound to the beads. Counting efficiency of the beads was not dependent upon the volume of the quenched mixture.

Rapid-quench experiments were conducted using a Kintec rapid-mixing apparatus (Johnson 1986). Preformed Enzyme•FPP (45 μL) was mixed with 45 μL of BiopepSH in the reaction buffer described above and quenched with 185 μL of stop reagent. An aliquot (40 μL) of the quenched mixture was analyzed as above.

Active Site Concentration. The concentration of active sites was estimated from the burst amplitude of a reaction of limiting FTase with 220 nM FPP and 2 μM BiopepSH.

Fluorescence Measurements. Fluorescence of FTase was monitored at an excitation wavelength of 280 nm and an emission wavelength of 325 nm with a Kontron SFM 25 fluorometer. Stopped-flow fluorescence was monitored with an Applied Photophysics stopped-flow instrument at an excitation wavelength of 280 nm and detection of emission scattering. FTase (40 nM) was mixed with FPP (0.020−20 μM) and/or 0.4−60 μM BiopepSH in 50 mM Tris, pH 7.7, 5 mM $MgCl_2$, 5 μM $ZnCl_2$, 2% DMSO, and 2 mM DTT at 25 °C.

Equations for Analysis of Kinetic Data. Equation 1 describes the dependence of the steady-state velocity on substrate concentration for a two-substrate random-equilibrium mechanism for FTase with FPP and BiopepSH to form BiopepS-C_{15}. K_F and K_B are the K_m values for FPP and BiopepSH at infinite second substrate, respectively; K_{FB} is K_FK_B; v is the velocity of product formation; and E_t is the total enzyme concentration.

$$\frac{v}{E_t} = \frac{k_{cat}[FPP][BiopepSH]}{[FPP][BiopepSH] + K_B[FPP] + K_F[BiopepSH] + K_{FB}} \quad (1)$$

Equation 2 describes the binding of FTase (E) to FPP in a two-step process where K_s is an equilibrium dissociation constant and k_1 and k_{-1} are forward and reverse rate constants, respectively, for a conformational change.

$$E + FPP \overset{K_s}{\rightleftharpoons} E{\cdot}FPP \underset{k_{-1}}{\overset{k_1}{\rightleftharpoons}} E{\cdot}FPP^* \quad (2)$$

The formation of E•FPP* from E and FPP is a pseudo-first-order process defined by eq 3, provided that [FPP] ≫ [E], E(FTase) and E•FPP have the same protein fluorescence, and E•FPP* has enhanced fluorescence:

$$k_{obs} = \frac{k_1[FPP]}{[FPP] + K_s} + k_{-1} \quad (3)$$

If [FPP] ≪ K_s, then eq 3 simplifies to eq 4a:

$$k_{obs} = k'_1[FPP] + k_{-1} \quad (4a)$$

and the second-order association rate constant for FTase and FPP (k'_1 in eq 4a) is approximated by eq 4b.

$$k'_1 = k_1/K_s \quad (4b)$$

Equation 5 is an ordered bi-bi reaction mechanism wherein the reaction of the second substrate (BiopepSH) with the enzyme−first substrate complex is second-order and functionally irreversible.

$$E + FPP \underset{k_{-1}}{\overset{k'_1}{\rightleftharpoons}} E{\cdot}FPP^* \xrightarrow{k_2[BiopepSH]} E{\cdot}BiopepS\text{-}C_{15} \xrightarrow{k_{cat}} E + BiopepS{-}C_{15} \quad (5)$$

For the kinetic mechanism of eq 5, the steady-state kinetic constants of eq 1 can be described in terms of the individual rate constants in eq 5 as follows: $K_B = k_{cat}/k_2$, $K_F = k_{cat}/k'_1$, and $K_{FB} = (k_{-1}k_{cat})/(k_1k_2)$. This is in contrast to the random equilibrium reaction mechanism where $K_{FB} = K_FK_B$.

Equation 6 describes the dependence of k_{obs} (the rate constant for the reaction of BiopepSH with FTase•FPP*) on [BiopepSH].

$$k_{obs} = k_2[BiopepSH] \quad (6)$$

Statistical Analysis. The parameters of the linear equations were determined by standard or weighted linear regression analysis. The parameters of the nonlinear equations were estimated with Sigma Plot (Jandel Scientific, Corte Madera, CA). Pseudo-first-order rate constants determined from stopped-flow data were estimated by the fitting routine included with the Applied Photophysics instrument. Error estimates were from the error matrix generated during the fitting routines. Error estimates for values calculated from fitted values (for example, calculated K_d values) were determined by the propagation of error analysis (Bevington, 1969).

RESULTS

Steady-state kinetic and isotope-trapping analyses of FTase demonstrated that FTase binds either Ras or isoprenyl pyrophosphate independently, but preferentially utilizes FTase•isoprenyl-PP (Pompliano et al. 1992, 1993). We examined steady-state kinetic parameters of FTase with the biotinylated heptapeptide (BiopepSH) and FPP as substrates and found similar results (Figure 1). Equation 1 was fit to the data with $K_F = 3.9 \pm 0.3$ nM, $K_B = 340 \pm 30$ nM, and $k_{cat} = 0.061 \pm 0.002$ s^{-1}. Since the kinetic constants determined from steady-state kinetic analysis do not unambiguously define the rate constants for the individual steps of an enzyme reaction, we also acquired pre-steady-state data by monitoring substrate-induced changes in enzyme fluorescence and by rapid quench experiments.

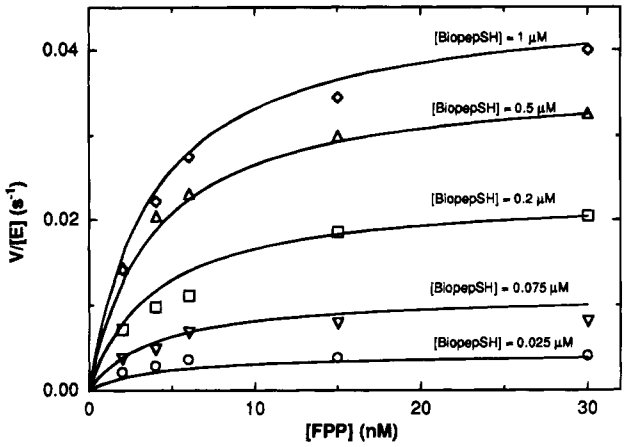

FIGURE 1: Steady-state kinetics of FTase-catalyzed farnesylation of BiopepSH with FPP. The steady-state initial velocities are expressed as rate constants (normalized for enzyme concentration). The solid lines were calculated with eq 1 and values for K_F of 3.9 ± 0.3 nM and K_B of 340 ± 30 nM.

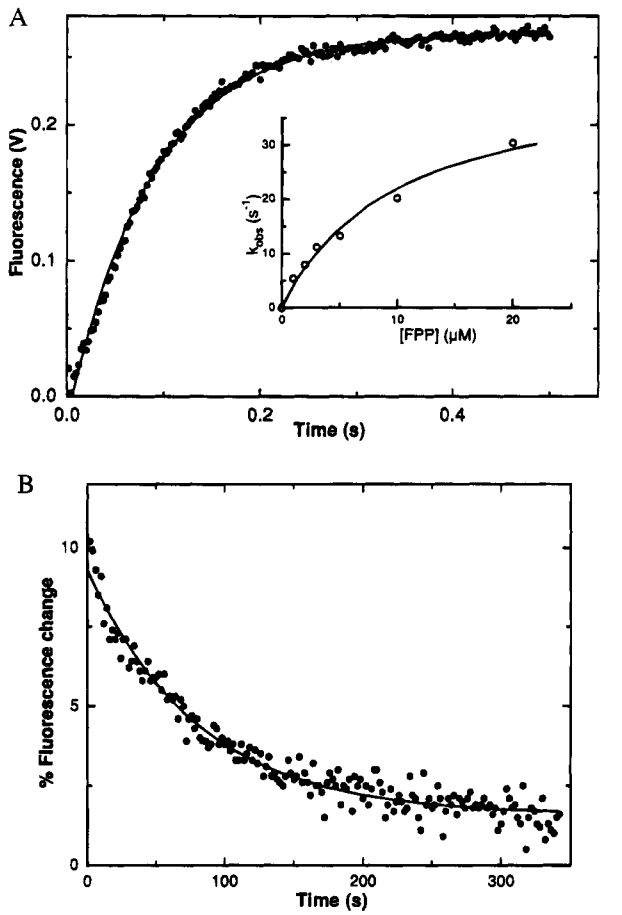

FIGURE 2: Rate constants for association and dissociation of FPP and FTase. (A) Protein fluorescence increase that occurs upon association of 0.020 μM FTase and 1 μM FPP. The solid line was calculated from a first-order process with a rate constant of 11.3 ± 0.1 s^{-1}. Inset: Concentration dependence of the rate constant for the FPP-induced fluorescence increase. The solid line was calculated with eq 3 and values for k_{-1} fixed at 0.013 s^{-1}, $K_s = 10 \pm 2$ μM, and $k_1 = 44 \pm 5$ s^{-1}. (B) Fluorescence decrease that occurs upon addition of 600 units of alkaline phosphatase to a mixture of 20 nM FTase and 70 nM FPP in 1.5 mL. The solid line was calculated from a first-order process with the rate constant of 0.0125 ± 0.0005 s^{-1}.

The protein fluorescence of FTase was increased 13% by 1 μM FPP (Figure 2A). The pseudo-first-order rate constant (k_{obs}) for formation of the binary complex from 1 μM FPP and 20 nM FTase was 11.3 ± 0.1 s^{-1}.[2] k_{obs} increased with the concentration of FPP to a maximal value (k_1) of 44 ± 5 s^{-1}. k_{obs} was half-maximal at 10 ± 2 μM FPP (which was the K_s) (Figure 2A). These data indicate that FTase bound FPP in a two-step process (eq 2). Furthermore, because the amplitude of the fluorescence change was similar over the concentration range of FPP used (data not shown), the equilibrium state of the enzyme was saturated as FTase•FPP* over that concentration range. Therefore, the overall K_d was much less than 1 μM (the lowest concentration tested), and the effective dissociation rate constant was much less than 11 s^{-1}. The effective dissociation rate constant (k_{-1}) for FTase•FPP* was determined to be 0.0125 ± 0.0005 s^{-1} by monitoring the decrease in protein fluorescence upon addition of alkaline phosphatase, which hydrolyzed any FPP that dissociated from FTase•FPP* (Figure 2B).[3] Thus, the overall dissociation constant (K_d) of FTase for FPP, which is $K_s(k_{-1}/(k_1 + k_{-1}))$, was 2.8 ± 0.6 nM.

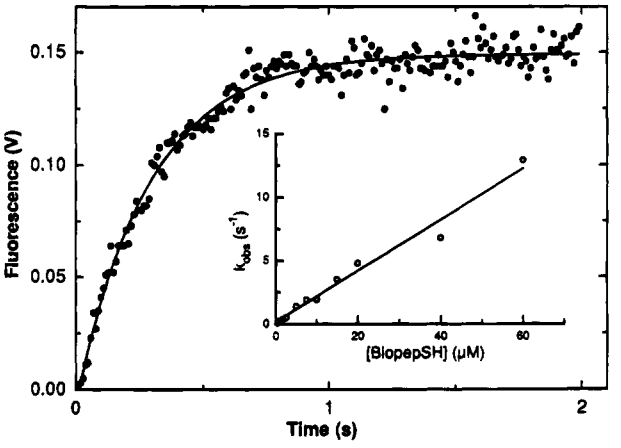

FIGURE 3: Reaction of BiopepSH with FTase•FPP, measured as fluorescence increase, monitored by stopped-flow, that occurs upon mixing 20 μM BiopepSH with 0.020 μM FTase and 1 μM FPP, as described in Materials and Methods. The solid line was calculated from a first-order process with a rate constant of 4.8 ± 0.1 s^{-1}. Inset: Dependence of the rate constant for BiopepSH-induced fluorescence increase in FTase•FPP on the concentration of BiopepSH. The solid line was calculated with eq 6 and a value for k_2 of (2.2 ± 0.1) × 10^5 M^{-1} s^{-1}.

BiopepSH (20 μM) increased the protein fluorescence of FTase•FPP* by 4% in a pseudo-first-order process. The rate constant (k_{obs}) was 4.8 ± 0.1 s^{-1} (Figure 3). k_{obs} was linearly dependent upon BiopepSH concentrations from 0 to 60 μM. The second-order rate constant (k_2) for association of BiopepSH to FTase•FPP* was (2.2 ± 0.1) x 10^5 M^{-1} s^{-1}

[2] FTase active site concentrations were determined by the amplitude of the burst in product formation when enzyme was reacted with saturating FPP and BiopepSH. Enzyme concentration was also estimated by quantitative amino acid analysis and by titration of the FTase fluorescence with FPP. These latter methods yielded values for enzyme concentration approximately 2.8-fold larger than the value obtained from the burst in product formation. This result suggested that 1/3 of the FPP binding sites were catalytically active. However, the discrepancies among determinations of enzyme concentration were not large enough to affect the conclusions of this study. For example, if the enzyme concentration determined from the latter methods is assumed, k_{cat} = 0.022 s^{-1}, and the calculated values for K_F, K_B, and K_{FB}, are 5.4 nM, 100 nM, and 320 nM^2, respectively (compare values in Table 1).

[3] Alkaline phosphatase effectively "trapped" FPP dissociated from FTase•FPP* by hydrolysis of the pyrophosphate bond. FPP added to a mixture of FTase and alkaline phosphatase yielded less than 10% of the fluorescence increase observed in the absence of alkaline phosphatase, indicating that free FPP was hydrolyzed by alkaline phosphatase before binding to FTase.

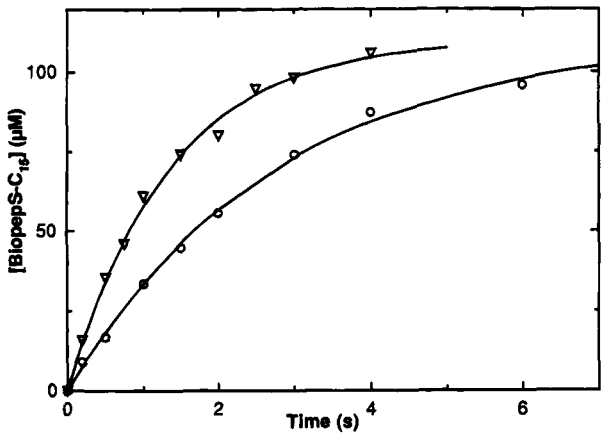

FIGURE 4: FTase (150 nM) and 110 nM [^{3}H]FPP formed FTase•[^{3}H]FPP (110 nM), which was reacted with 2 μM (○) or 4 μM (▽) BiopepSH with a rapid quench instrument, as described in Materials and Methods. The solid lines were calculated from a first-order process and rate constants equal to 0.036 ± 0.002 and 0.075 ± 0.004 s^{-1} for 2 and 4 μM BiopepSH, respectively.

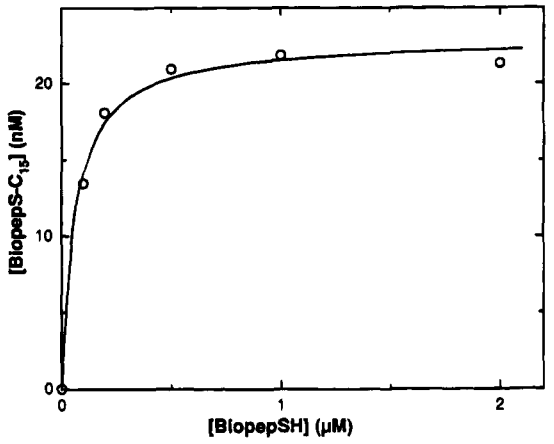

FIGURE 5: Trapping of enzyme-bound FPP with BiopepSH. FTase (27 nM) and 22 nM [^{3}H]FPP were mixed to form 22 nM FTase•[^{3}H]FPP, and the complex was reacted with a mixture of BiopepSH (0.1−2 μM) and 2 μM unlabeled FPP. The solid line was calculated from eq 7 (in Results) and values for P_{max} of 22.9 ± 0.6 nM and $K_{1/2}$ of 0.062 ± .009 μM.

(Figure 3, inset). Because the value of the *y*-intercept of this plot was not significantly different from zero (0.02 ± 0.01 s^{-1}), the reaction of peptide with FTase•FPP* was functionally irreversible. Two possible explanations for this result are (1) the dissociation of BiopepSH was slow, and (2) a rapid and irreversible event, such as chemistry to form the enzyme-bound farnesylated peptide product, follows binding of the peptide, thus trapping the peptide and FPP. To distinguish between these possibilities, rate constants for a single turnover of FTase•FPP* were determined as a function of peptide concentration.

Using a rapid quench instrument, 2 or 4 μM BiopepSH was reacted with 110 nM FTase•FPP* and resulted in first-order formation of product with k_{obs} values of 0.36 ± 0.02 and 0.75 ± 0.04 s^{-1}, respectively (Figure 4). k_{obs} values for association of 2 and 4 μM BiopepSH with FTase•FPP* were 0.44 and 0.88 s^{-1}, respectively (Figure 3), and were essentially the same as the k_{obs} values for a single turnover at these concentrations of BiopepSH. These data indicate that (1) the reaction of BiopepSH with FTase•FPP* to form enzyme-bound product was a second-order process, (2) formation of enzyme-bound product from the ternary complex must have occurred rapidly compared to association and dissociation of the peptide at these concentrations, (3) the FTase−product complex has increased fluorescence compared to FTase•FPP*, (4) k_{obs} for the fluorescence increase of BiopepSH binding FTase•FPP* is a measure of FTase-product complex, and (5) an enzyme equivalent of product is formed with a rate constant of at least 0.8 s^{-1}, and perhaps as large as 12 s^{-1} (see Figure 3).[4]

The dissociation rate constant for E•FPP was independently measured by the isotope-trapping method of Rose (Pompliano et al., 1993; Rose et al., 1974). FTase•[^{3}H]FPP (22 nM) was generated by mixing FTase (27 nM) and 22 nM [^{3}H]-FPP. The complex was reacted with a mixture of BiopepSH (0.1−2 μM) and 2 μM unlabeled FPP (Figure 5). The amount of product formed from FTase•[^{3}H]-FPP, as a function of [BiopepSH] (P(B)), is given by eq 7, where $K_{1/2}$ is the concentration of BiopepSH which gives one-half the maximal possible product formed, and P_{max} is the maximal amount of product formed at saturating [BiopepSH].

$$P(B) = \frac{P_{max}[\text{BiopepSH}]}{[\text{BiopepSH}] + K_{1/2}} \quad (7)$$

$K_{1/2}$ is further defined by eq 5 as the [BiopepSH] which gives k_2[BiopepSH] = k_{-1}. P_{max} is further defined by eq 5 as the amount of product formed when k_2[BiopepSH] ≫ k_{-1}. Equation 7 was fit to the data (Figure 5) to give a P_{max} of 22.9 ± 0.6 nM and a $K_{1/2}$ for BiopepSH of 0.062 ± 0.009 μM. k_{-1}, which equals $k_2K_{1/2}$, was calculated to be 0.014 ± 0.002 s^{-1} from $K_{1/2}$ and k_2 ((2.2 ± 0.1) × 10^5 M^{-1} s^{-1}). This value for k_{-1} is similar to that determined by enzyme fluorescence changes (0.0125 ± 0.0005 s^{-1}). Furthermore, because P_{max} was not significantly different from the concentration of FTase•FPP*, product formation was functionally irreversible, indicating that FPP did not dissociate from the ternary complex.

We then examined the interaction of BiopepSH with free enzyme. The fluorescence of FTase was increased 8% by BiopepSH (4 μM) with a rate constant (k_{obs}) of 0.046 ± 0.003 s^{-1} (data not shown). k_{obs} did not depend upon BiopepSH concentration (the range of rate constants determined from 0.5 to 16 μM BiopepSH was 0.038−0.048 s^{-1}). However, the amplitude of the fluorescence change was dependent upon BiopepSH concentration with a maximal increase of 11% and a half-maximal increase at 1.0 ± 0.3 μM BiopepSH (K_d for FTase and BiopepSH). Other peptide substrates, such as GLPCVVM (without the N-terminal biotin) and TKCVIM induced similar fluorescence changes in FTase (data not shown). In contrast, TKSVIM, a peptide that does not bind FTase significantly as a substrate or an inhibitor (Chen et al. 1993), did not induce a fluorescence change in FTase. Together, these results suggest that the interactions of BiopepSH with free FTase were specific for binding the active site.

Because these data indicated binding of BiopepSH to free FTase, we attempted to trap the enzyme-bound BiopepSH with 310 nM [^{3}H]FPP in the presence of a 50-fold excess of competitor peptide (GLPCVVM). Enzyme-bound peptide was not trapped by FPP, which suggests either that the

[4] It was desirable to verify that product formation from FTase•FPP occurred as fast as the enzyme fluorescence changes at BiopepSH concentrations higher than 4 μM used herein. However, due to the limited BiopepSH-binding capacity of the streptavidin beads used for the assay, this was not readily possible.

Table 1: Kinetic Constants for FTase

constant[a]	exptl value	calcd value
K_F	3.8 ± 0.8 nM[b] 3.9 ± 0.3 nM[c]	15 ± 4 nM[b]
K_B	330 ± 60 nM[b] 340 ± 30 nM[c]	280 ± 20 nM[b]
K_{FB}	1300 ± 300 nM[2 b]	900 ± 200 nM[2 b]
k_{cat}	0.061 ± 0.004 s^{-1}	
K_s	10 ± 2 μM	
k_1	44 ± 5 s^{-1}	
k_{-1}	0.0125 ± 0.0005 s^{-1} [d] 0.014 ± 0.002 s^{-1} [e]	
$K_{d(FPP)}$		2.8 ± 0.6 nM
k'_1		$(4 \pm 1) \times 10^6$ M^{-1} s^{-1}
k_2	$(2.2 \pm 0.1) \times 10^5$ M^{-1} s^{-1}	

[a] K_F, K_B, K_{FB}, and k_{cat} are defined by eq 1; K_s, k_1, and k_{-1} are defined by eq 2; k'_1 and k_2 are defined by eq 5; and $K_{d(FPP)} = K_s(k_{-1}/(k_1 + k_{-1}))$. Equations are defined in Materials and Methods. [b] Value determined by fit of eq 1 to the steady-state data or calculated, assuming eq 5 as the kinetic mechanism, i.e., $K_B = k_{cat}/k_2$, $K_F = k_{cat}/k'_1$, $K_{FB} = (k_{-1}k_{cat})/(k_1k_2)$. [c] Value determined by fit of eq 1 to the steady-state data, assuming a random equilibrium model, i.e., $K_{FB} = K_FK_B$. [d] Value determined by protein fluorescence changes upon dissociation of FPP. [e] Value determined by trapping of [^{3}H]-FPP from FTase·[^{3}H]-FPP reaction with BiopepSH.

peptide dissociates with a rate constant much greater than 1.4 s^{-1} (which is the rate constant for association of 310 nM FPP) or that the enzyme–peptide complex is not in a reactive conformation. Furthermore, these data indicate that FTase·BiopepSH is not utilized in catalysis.

These data in total allowed us to propose the minimal kinetic scheme of eq 5. The pre-steady-state and steady-state rate constants for FTase are summarized in Table 1. The steady-state constants calculated from the individual rate constants, assuming the kinetic mechanism of eq 5, were similar to the values determined by steady-state analysis.

DISCUSSION

Previous analysis of steady-state kinetic parameters for FTase with several isoprenyl and Ras protein substrates, coupled with an isotope-trapping experiment, suggested a functionally ordered mechanism for the enzyme with FPP binding first (Pompliano et al., 1993). In the present study, we determined the steady-state kinetic parameters for the FTase reaction using a synthetic biotinylated heptapeptide substrate (BiopepSH) which is similar to the Ras-CVIM protein used by Pompliano et al. (1993). This steady-state kinetic analysis gave results similar to those of Pompliano et al. (1993), confirming that a small peptide substrate can be used in a kinetic analysis of the enzyme.

Because steady-state analysis cannot unambiguously determine the individual rate constants which describe a kinetic mechanism, we determined the pre-steady-state kinetic constants using rapid mixing techniques and stopped-flow fluorescence studies. Through these studies, we found that FPP binds FTase in a two-step process, with the second step apparently involving a conformational change in the enzyme–substrate complex. We also determined the dissociation rate constant for FTase·FPP* and, combining this with the observed association rate constants, calculated the overall K_d for formation of FTase·FPP* to be 2.8 nM. The apparent second order association rate constant for FPP (k'_1), which equals k_1/K_s, was calculated to be 4×10^6 M^{-1} s^{-1}. The approximation that k'_1 is the second-order association rate constant for FPP is only valid for concentrations of FPP well below K_s (which was 10 μM). Because the steady-state constants were determined with concentrations of FPP between 2 and 30 nM, defining FPP binding as a single step (eq 5) is valid.

Reaction of BiopepSH with FTase·FPP* to form FTase·BiopepS-C_{15} was a second-order process with a rate constant (k_2) of 2.2×10^5 M^{-1} s^{-1}. This rate constant is small compared to values typical of small molecules associating with enzymes, which are on the order of 10^6–10^8 M^{-1} s^{-1} (Fersht, 1985). However, in the case of FTase, k_2 is the rate constant for a second-order chemical reaction. Therefore, it is not surprising that its magnitude is smaller than typical association rate constants for substrates with enzymes. On the basis of the value for k_2, at 2 μM BiopepSH (which is $6K_B$), the rate constant for conversion of FTase·FPP* to FTase·BiopepS-C_{15} was 0.44 s^{-1}. Since k_{cat} was 0.06 s^{-1}, the formation of enzyme-bound product (FTase·BiopepS-C_{15}) at 2 μM BiopepSH occurs 7.3 times faster than the maximal rate of product formation. Therefore, product release is the rate-determining step under steady-state conditions and at saturating substrate concentrations. It is also possible that product dissociation is rapid but is followed by a slow conformational change; however, we do not have evidence to suggest such a mechanism.

Many enzymes show rate-determining product release. Examples include several dehydrogenases where NADH release is rate-determining (Fersht 1985), single nucleotide incorporation by reverse transcriptase where the extended template primer release is rate-determining (Reardon, 1992), and amino acid oxidation by both L-amino acid oxidase and D-amino acid oxidase (Bright & Porter 1975). Interestingly, both reverse transcriptase and alcohol dehydrogenase also catalyze reactions by ordered kinetic mechanisms (Dalziel, 1975; Reardon, 1992) similar to FTase.

When displacement reactions involving small molecules occur with second-order kinetics, the mechanism is generally thought to involve an S_N2 or "S_N2 like" transition state. In the case of the reaction studied here, this would involve the sulfhydryl group of the substrate peptide directly displacing the pyrophosphate of FPP. While the reaction of BiopepSH with FTase·FPP* to form FTase·BiopepS-C_{15} is a second-order process, it is likely that the enzyme-catalyzed reaction has a binding step for substrate peptide that precedes the chemical reaction. The binding step may not be experimentally detected because the K_d for BiopepSH binding to FTase·FPP* may be very high or the chemical reaction in the ternary complex may be very fast compared to dissociation of BiopepSH from the ternary complex. Because a peptide-binding step likely precedes the chemical step on the enzyme, our kinetic analysis does not rigorously define the molecularity of the chemical step as S_N2, although it may be S_N2. Displacements that occur at carbons adjacent to allylic carbons often utilize carbonium ion (S_N1) mechanisms (i.e., the bond is acid labile). Furthermore, enzymes such as isopentenyl pyrophosphate isomerase utilize carbonium ion mechanisms (Reardon & Abeles, 1986; Muehlbacher & Poulter, 1988). Therefore, it is possible that FTase utilizes a carbonium ion mechanism. One further possibility is that the mechanism of FTase proceeds through an "exploded transition state" (Jencks, 1981, 1985), such that carbonium

ion character has developed on C_1 of FPP in the transition state, even though the mechanism is formally S_N2.

We used an isotope trapping technique (Pompliano et al., 1993; Rose et al., 1974) to obtain an independent measure of k_{-1} and to determine the commitment to catalysis of FTase·FPP*. k_{-1}, determined by this method, was 0.014 s^{-1} and was similar to that determined by protein fluorescence changes (0.013 s^{-1}). Under conditions of saturating BiopepSH, all of the enzyme-bound FPP was converted to BiopepS-C_{15}. This result indicates that (1) FPP does not dissociate from the ternary complex, (2) the ternary complex does not have a significant lifetime, and (3) the reaction is functionally irreversible. Furthermore, in the presence of 1 μM BiopepSH (the maximum concentration of BiopepSH used in the steady-state analysis), FTase·FPP* partitions to product 17 times more frequently than it dissociates to FPP in the steady state. This result demonstrates that the FTase·FPP* is highly committed to catalysis, as suggested by Pompliano et al. (1993).

BiopepSH induced a fluorescence change in FTase. The amplitude of the fluorescence change decreased with decreasing [BiopepSH], giving an apparent K_d of 1 μM for BiopepSH and free FTase. Interestingly, the rate constant for association of BiopepSH (0.4 s^{-1}) did not change significantly with [BiopepSH]. One possible explanation for these results is that FTase exists in two conformations (with one species accounting for over 90% of the enzyme) which slowly interconvert and that BiopepSH rapidly binds to the major species of FTase with a K_d of 1 μM [see Fersht (1985)]. Enzyme-bound BiopepSH could not be trapped by FPP. This result suggests either that BiopepSH dissociated from the binary complex faster than product formation or that BiopepSH bound free FTase as a nonproductive complex. Furthermore, this result demonstrates that FTase·BiopepSH is not utilized in catalysis.

The rate constants that describe the kinetic scheme of eq 5 were determined from pre-steady-state data, isotope trapping data, and steady-state data. The steady-state kinetic constants (K_F, K_B, and K_{FB}) calculated from these rate constants were similar to those determined from steady-state analysis (Table 1). This result indicated that the simple, ordered kinetic mechanism defined by eq 5 was sufficient to explain the kinetics of FTase-catalyzed farnesylation of BiopepSH.

In summary, FTase catalyzes the farnesylation of BiopepSH with an ordered kinetic mechanism which involves FPP binding first. FPP binds FTase in a two-step process that may involve an enzyme conformational change. BiopepSH then reacts with FTase·FPP in a functionally irreversible, second-order process to form FTase·BiopepS-C_{15}. Product release from FTase·BiopepS-C_{15} is the rate-determining step (k_{cat}) during steady-state catalysis at saturating substrate concentrations.

ACKNOWLEDGMENT

We thank D. Porter and J. Reardon for helpful comments and discussions during the course of this work; B. Merrill and W. Chestnut for the quantitative amino acid analysis; and T. Spector, T. Zimmerman, and T. Krenitsky for their continued support.

REFERENCES

Bevington, P. R. (1969) *Data Reduction and Error Analysis for the Physical Sciences*, pp 56–65, McGraw-Hill Inc., New York.
Bright, H. J., & Porter D. J. T. (1975) *Enzymes (3rd Ed.) 12*, 421–505.
Casey, P. J. (1994) *Curr. Opin. Cell Biol. 6*, 219–225.
Chen, W.-J., Andres, D. A., Goldstein, J. L., & Brown, M. S. (1991a) *Proc. Natl. Acad. Sci. U.S.A. 88*, 11368–11372.
Chen, W.-J., Andres, D. A., Goldstein, J. L., Russell, D. W., & Brown, M. S. (1991b) *Cell 66*, 327–334.
Chen, W.-J., Moomaw, J. F., Overton, L., Kost, T. A., & Casey, P. J. (1993) *J. Biol. Chem. 268*, 9675–9680.
Clarke, S. (1992) *Annu. Rev. Biochem. 61*, 355–386.
Dalziel, K. (1975) *Enzymes (3rd Ed.) 11*, 1–60.
Fersht, A. (1985) *Enzyme Structure and Mechanism*, 2nd ed., pp 121–155, W. H. Freeman and Co., New York.
Gibbs, J. B., Oliff, A., & Kohl, N. E. (1994) *Cell 77*, 175–178.
Goldstein, J. L., Brown, M. S., Stradley, S. J., Reiss, Y., & Gierasch, L. M. (1991) *J. Biol. Chem. 266*, 15575–15578.
James, G. L., Goldstein, J. L., Brown, M. S., Rawson, T. E., Somers, T. C., McDowell, R. S., Crowley, C. W., Lucas, B. K., Levinson, A. D., & Marsters, J. C., Jr. (1993) *Science 260*, 1937–1942.
Jencks, W. P. (1981) *Chem. Soc. Rev. 10*, 345–375.
Jencks, W. P. (1985) *Chem. Rev. 85*, 511–527.
Johnson, K. A. (1986) *Methods Enzymol. 134*, 677–705.
Kohl, N. E., Diehl, R. E., Schaber, M. D., Rands, E., Soderman, D. D., He, B., Moores, S. L., Pompliano, D. L., Ferro-Novick, S., Powers, S., Thomas, K. A., & Gibbs, J. B. (1991) *J. Biol. Chem. 266*, 18884–18888.
Kohl, N. E., Mosser, S. D., deSolms, S. J., Giuliani, E. A., Pompliano, D. L., Graham, S. L., Smith, R. L., Scolnick, E. M., Oliff, A., & Gibbs, J. B. (1993) *Science 260*, 1934–1937.
Kohl, N. E., Wilson, F. R., Mosser, S. D., Giuliani, E., deSolms, S. J., Conner, M. W., Anthony, N. J., Holtz, W. J., Gomez, R. P., Lee, T.-J., Smith, R. L., Graham, S. L., Hartman, G. D., Gibbs, J. B., & Oliff, A. (1994) *Proc. Natl. Acad. Sci. U.S.A. 91*, 9141–9145.
Merrifield, R. B. (1963) *J. Am. Chem. Soc. 85*, 2149–2154.
Moores, S. L., Schaber, M. D., Mosser, S. D., Rands, E., O'Hara, M. B., Garsky, V. M., Marshall, M. S., Pompliano, D. L., & Gibbs, J. B. (1991) *J. Biol. Chem. 266*, 14603–14610.
Muehlbacher, M., & Poulter, C. D. (1988) *Biochemistry 27*, 7315–7328.
Omer, C. A., Kral, A. M., Diehl, R. E., Prendergast, G. C., Powers, S., Allen, C. M., Gibbs, J. B., & Kohl, N. E. (1993) *Biochemistry 32*, 5167–5176.
Pompliano, D. L., Rands, E., Schaber, M. D., Mosser, S. D., Anthony, N. J., & Gibbs, J. B. (1992) *Biochemistry 31*, 3800–3807.
Pompliano, D. L., Schaber, M. D., Mosser, S. D., Omer, C. A., Shafer, J. A., & Gibbs, J. B. (1993) *Biochemistry 32*, 8341–8347.
Reardon, J. E. (1992) *Biochemistry 31*, 4473–4479.
Reardon, J. E., & Abeles, R. H. (1986) *Biochemistry 25*, 5609–5616.
Reiss, Y., Goldstein, J. L., Seabra, M. C., Casey, P. J., & Brown, M. S. (1990) *Cell 62*, 81–88.
Reiss, Y., Seabra, M. C., Armstrong, S. A., Slaughter, C. A., Goldstein, J. L., & Brown, M. S. (1991a) *J. Biol. Chem. 266*, 10672–10677.
Reiss, Y., Stradley, S. J., Gierasch, L. M., Brown, M. S., & Goldstein, J. L. (1991b) *Proc. Natl. Acad. Sci. U.S.A. 88*, 732–736.
Rose, I. A., O'Connell, E. L., Litwin, S., & Tana, J. B. (1974) *J. Biol. Chem. 249*, 5163–5168.
Stewart, J. M., & Young, J. D. (1984) *Solid Phase Peptide Synthesis*, 2nd ed., Pierce Chemical Co., Rockfort, IL.

BI942598R